

1 **Positive selection in the genomes of two Papua New Guinean populations at**
2 **distinct altitude levels**

3 Mathilde André¹, Nicolas Brucato², Georgi Hudjasov³, Vasili Pankratov³, Danat
4 Yermakovich³, Rita Kreevan³, Jason Kariwiga^{4,5}, John Muke⁶, Anne Boland⁷, Jean-
5 François Deleuze⁷, Vincent Meyer⁷, Nicholas Evans⁸, Murray P. Cox⁹, Matthew
6 Leavesley^{10,11}, Michael Dannemann³, Tõnis Org³, Mait Metspalu¹, Mayukh
7 Mondal^{3,12*}, François-Xavier Ricaut^{2*}

8 *These authors contributed equally

9 Corresponding authors:

10 mondal.mayukh@gmail.com

11 francois-xavier.ricaut@univ-tlse3.fr

12 **Affiliations:**

- 13 1. Estonian Biocentre, Institute of Genomics, University of Tartu, Riia 23b, 51010 Tartu,
14 Tartumaa, Estonia
- 15 2. Laboratoire Évolution and Diversité Biologique (EDB UMR5174), Université de
16 Toulouse Midi-Pyrénées, CNRS, IRD, UPS, Toulouse, France
- 17 3. Centre for Genomics, Evolution & Medicine, Institute of Genomics, University of
18 Tartu, Riia 23b, 51010 Tartu, Tartumaa, Estonia
- 19 4. Strand of Anthropology, Sociology and Archaeology, School of Humanities and Social
20 Sciences, University of Papua New Guinea, PO Box 320, University 134, National
21 Capital District, Papua New Guinea
- 22 5. School of Social Science, University of Queensland, St Lucia, Queensland, Australia
- 23 6. Social Research Institute Ltd, Port Moresby, Papua New Guinea
- 24 7. Université Paris-Saclay, CEA, Centre National de Recherche en Génomique
25 Humaine (CNRGH), 91057, Evry, France
- 26 8. ARC Centre of Excellence for the Dynamics of Language, Coombs Building, Fellows
27 Road, CHL, CAP, Australian National University, Australia
- 28 9. School of Natural Sciences, Massey University, Palmerston North, New Zealand.
- 29 10. College of Arts, Society and Education, James Cook University, P.O. Box 6811,
30 Cairns, Queensland, 4870, Australia
- 31 11. ARC Centre of Excellence for Australian Biodiversity and Heritage, University of
32 Wollongong, Wollongong, New South Wales, 2522, Australia
- 33 12. Institute of Clinical Molecular Biology, Christian-Albrechts-Universität zu Kiel 24118
34 Kiel, Germany

35 **Keywords**

36 Selection, altitude, New Guinea, hypoxia, introgression

37 Abstract

38 Highlanders and lowlanders of Papua New Guinea (PNG) have faced distinct
39 environmental conditions. These environmental differences lead to specific stress on
40 PNG highlanders and lowlanders, such as hypoxia and environment-specific pathogen
41 exposure, respectively. We hypothesise that these constraints induced specific
42 selective pressures that shaped the genomes of both populations. In this study, we
43 explored signatures of selection in newly sequenced whole genomes of 54 PNG
44 highlanders and 74 PNG lowlanders. Based on multiple methods to detect selection,
45 we investigated the 21 and 23 genomic top candidate regions for positive selection in
46 PNG highlanders and PNG lowlanders, respectively. To identify the most likely
47 candidate SNP driving selection in each of these regions, we computationally
48 reconstructed allele frequency trajectories of variants in each of these regions and
49 chose the SNP with the highest likelihood of being under selection with CLUES. We
50 show that regions with signatures of positive selection in PNG highlanders genomes
51 encompass genes associated with the hypoxia-inducible factors pathway, brain
52 development, blood composition, and immunity, while selected genomic regions in
53 PNG lowlanders contain genes related to immunity and blood composition. We found
54 that several candidate driver SNPs are associated with haematological phenotypes in
55 the UK biobank. Moreover, using phenotypes measured from the sequenced Papuans,
56 we found that two candidate SNPs are significantly associated with altered heart rates
57 in PNG highlanders and lowlanders. Furthermore, we found that 16 of the 44 selection
58 candidate regions harboured archaic introgression. In four of these regions, the
59 selection signal might be driven by the introgressed archaic haplotypes, suggesting a
60 significant role of archaic admixture in local adaptation in PNG populations.

61 Introduction

62 After the first arrival of modern humans in New Guinea around 50 thousand years ago
63 (kya) ^{1,2}, they rapidly spread across different environmental niches of the island ^{3,4}.
64 Since the Holocene (around 11 kya), the Papua New Guinea (PNG) population has
65 been unevenly distributed, with most of the population living at altitude between 1600
66 and 2400 meters above sea level (a.s.l.) ⁵⁻⁷. This population distribution pattern is
67 remarkable considering the challenges PNG highlanders face at this altitude, like the
68 lower oxygen availability to the body ⁸. Studies investigating hypoxic response of the
69 human body in high-altitude populations revealed that selection acted on genes
70 involved in the Hypoxia-Inducible Factor (HIF)-pathway^{9,10}, the principal response
71 mechanism to low oxygen at the cellular level. It regulates angiogenesis,
72 erythropoiesis, and glycolysis ¹¹. Some high-altitude populations show a limited
73 increase in haemoglobin concentration ¹² in response to the lower oxygen levels.
74 Indeed, an increase in haemoglobin concentration – as observed in native lowlanders
75 accessing altitude – increases oxygen transport but also results in higher blood
76 viscosity ¹³. In the long term, that process may cause Chronic Mountain Sickness
77 (CMS) and cardiovascular complications ¹³. Interestingly, Tibetan highlanders show
78 selection that is associated with a more restrained increase of haemoglobin
79 concentration at altitude due to increased plasma volume ¹⁴. This suggests that
80 hypoxia might lead to the selection of a complex haematological response that
81 overcomes the increase in blood viscosity when enhancing oxygen transport.
82 However, the role of selection in response to the environmental challenges by altitude
83 on the genomes of PNG highlanders, who inhabited this environment for the last
84 20,000 years ⁴, remains mostly unknown. PNG highlanders significantly differ from
85 PNG lowlanders in height, chest depth, haemoglobin concentration, and pulmonary
86 capacities ¹⁵. Similar differences have been observed between Andean, Tibetan and
87 Ethiopian highlanders and their corresponding lowland populations ¹⁶. However
88 various factors, like phenotypic plasticity ¹⁷, diet or physical activities, could explain
89 these phenotype differences. In this paper we explored whether these phenotypes can
90 also be linked to adaptive processes acting on the genome of the PNG highlanders.

91 Other strong environmental pressures in PNG are infectious diseases (e.g., malaria,
92 dysentery, pneumonia, tuberculosis, etc) that are the leading cause of death in PNG
93 ¹⁸⁻²⁰. In this pathogenic environment, malaria stands out among others and could have

94 affected selective pressure in highlanders and lowlanders differently. Incidence of
95 malaria varies enormously between the lowlands and the highlands. While PNG
96 accounted for nearly 86% of the malaria cases in the Western Pacific Region in 2020
97 ²¹, malaria is practically absent in PNG highlands, possibly because of a limited
98 dispersal of *Anopheles*, the main vector of malaria, at high altitude ^{6,22}. It has been
99 suggested that malaria might explain the unbalanced population distribution between
100 PNG highlands and lowlands ^{7,23,24} and thus induces a selection pressure specific to
101 lowlanders. Nonetheless, the period when this specific pathogenic pressure started to
102 impact Papuans remains unclear.

103 Besides facing these environmental pressures, PNG populations also stand out by
104 their high levels of Denisovan introgression ^{25,26}. Denisovan introgressed variant might
105 contribute to Tibetans adaptation to altitude ²⁷ and affect the immune system of the
106 PNG population ²⁸. Moreover, because some archaic variants show signals of selection
107 among the overall Papuan population ^{29–31}, it is conceivable that archaic introgression
108 has contributed to beneficial alleles in PNG populations. However, to date it remains
109 elusive how to which extent archaic introgression contribution to local adaptation varies
110 between PNG populations.

111 In this study, we identify the genomic regions that show signatures of selection in 54
112 newly sequenced PNG highlanders and 74 lowlanders. We then screen for the SNP
113 that most likely drives the selection signal in each genomic region under selection. We
114 then explore phenotype associations with candidate SNPs. Finally, we scan selection
115 candidate regions for the presence of introgressed archaic haplotypes and assess the
116 role of introgressed alleles on adaptive processes. Our research provides new insights
117 into local adaptation in PNG populations and its implications on health.

118

119 **Material and Methods**

120 **Ethics**

121 This study was approved by the Medical Research Advisory Committee of Papua New
122 Guinea under research ethics clearance MRAC 16.21 and the French Ethics
123 Committees (Committees of Protection of Persons CPP 25/21_3, n_S1 :
124 21.01.21.42754). Permission to conduct research in PNG was granted by the National
125 Research Institute (visa n°99902292358) with full support from the School of
126 Humanities and Social Sciences, University of Papua New Guinea. All samples were
127 collected from healthy unrelated adult donors who provided written informed consent.
128 After a full presentation of the project to a wide audience, a discussion with each
129 individual willing to participate ensured that the project was fully understood.

130 **Samples**

131 DNA was extracted from saliva samples with the Oragene sampling kit according to
132 the manufacturer's instructions. Sequencing libraries were prepared using the TruSeq
133 DNA PCR-Free HT kit. About 150-bp paired-end sequencing was performed on the
134 Illumina HiSeq X5 sequencer. We sequenced PNG whole genomes from PNG
135 lowlanders from Daru (n=38, <100 m above sea level (a.s.l)) and PNG highlanders
136 from Mount Wilhelm villages (n=46, 2,300 and 2,700 m a.s.l.) sampled between 2016
137 and 2019 (EGA accession code XXXXX). To increase our sample size, we included
138 58 published genomes sampled in Port Moresby, including individuals from different
139 regions in PNG ³. We also gained access to PNG whole genome sequences from
140 samples collected at the same sampling places during the same period and sequenced
141 at the National Center of Human Genomics Research (France) or the KCCG
142 Sequencing Laboratory (Garvan Institute of Medical Research, Australia) (unpublished
143 data; F-X. Ricaut personal communication). These additional datasets increased our
144 sample size to a total of 262 PNG whole genomes with 60 individuals from Mount
145 Wilhelm (PNG highlanders), 80 individuals from Daru (PNG lowlanders) and 122
146 individuals sampled in Port Moresby from different origins (PNG diversity set I) (Note
147 S1, Tables S1-S2). We measured phenotypes associated with body proportion,
148 pulmonary capacities and cardiovascular components in this PNG dataset ¹⁵ (Note S2,
149 Table S3).

150 We combined these 262 sequences with published Papuan genomes (n=81, PNG
151 diversity II) ^{30,32–35} and high-coverage genomes from the 1000 Genomes project from
152 Africa (n=207), East Asia (n=202) and Europe (n=190) ³⁶ (Note S1).

153 **Variant Calling**

154 Sequencing data for all samples used in this study were processed together, starting
155 from the raw reads. FASTQ files were trimmed with fastp v0.23.2 ³⁷ and converted to
156 BAM using Picard Tools FastqToSam v2.26.2 ³⁸. Further processing was performed
157 with Broad Institute's GATK Germline short variant discovery (SNPs and Indels) Best
158 Practices ³⁹. HaplotypeCaller tool was used to produce individual sample GVCF files,
159 which were further combined by JointGenotyping workflow to create multi-sample VCF
160 files. GATK v4.2.0.0 was used ⁴⁰. Data were processed with GRCh38 genome
161 reference (Note S3).

162 **Filtering**

163 Unless otherwise stated, we performed the analysis on biallelic SNPs with a maximal
164 missing rate of 5% that remained after genomic masking (Note S7). For each pair of
165 related individuals to the second degree, when relevant, we kept the individuals with
166 the highest number of phenotypes measurements or the individual with the highest
167 mean of coverage. We removed two PNG samples with low call rate from any further
168 analysis. Quality and kinship filtering resulted in 249 unrelated genomes among the
169 PNG highlanders, lowlanders and the PNG diversity set I: 54 sequences of PNG
170 highlanders, 74 sequences from PNG lowlanders and 121 sequences from individuals
171 originating from different parts of PNG and sampled in Port Moresby (PNG diversity
172 set I; Notes S1, S4-S7, Tables S1-S4, Figures S1-S2). The unrelated and filtered
173 dataset also includes 262 published Papuan sequences (n=81, PNG diversity II) ^{30,32–}
174 ³⁵ and sequences from the 1000 Genomes project from Africa (n=207), East Asia
175 (n=202) and Europe (n=190) ³⁶ (Note S1).

176 **Population structure**

177 Principal Component Analysis (PCA) was performed on the unrelated dataset filter for
178 variant with minor allele frequency <5% and pruned for linkage disequilibrium (Note
179 S8) using the smartpca program from the EIGENSOFT v.7.2.0 package ⁴¹. To prune
180 variants in high linkage disequilibrium, we used PLINK v.1.9 using the default
181 parameters of 50 variants count window shifting from five variants and a variance

182 inflation factor (VIF) threshold of 2⁴². The LD pruned dataset included 469,584 SNPs
183 (4,809,440 SNPs before pruning).

184 We used the R-3.3.0 software to plot the PCA. We computed the PCA to the tenth
185 principal component. We ran ADMIXTURE v1.3⁴³ on the same dataset from
186 components K=2 to K=6. To define how many components composed the most likely
187 model, we computed each component's confidence interval of the cross-validation
188 error by repeating it 50 times (Note S9).

189 **Phasing**

190 We phased genomes from Mt Wilhelm, Daru, PNG diversity set I, Africa, Asia and
191 Europe using shapeit4 (v4.2.2)⁴⁴. We phased the samples statistically without
192 reference, as the reference haplotypes panel for the PNG population does not exist
193 (Note S10).

194 **Selection analysis**

195 We aimed to identify genomic regions carrying signatures of positive selection in PNG
196 highlanders and lowlanders using three metrics. We computed Population Branch
197 Statistic (PBS), a method based on allele frequency, to detect recent natural selection
198 signals in PNG highlanders and lowlanders⁴⁵ (Note S11). For the PBS scores in PNG
199 highlanders, we used PNG lowlanders as reference and Yorubas (YRI) from 1000
200 Genome as the outgroup. When performing PBS on PNG lowlanders, we used PNG
201 highlanders as reference and the YRI as the outgroup. In both cases, we obtained a
202 PBS score for every biallelic SNP. We then defined sliding windows of 20 SNPs with a
203 step of 5 SNPs to identify multiple adjacent SNPs with an elevated PBS score (which
204 lowers the random chances due to drift). We assigned the average PBS score of all
205 the SNPs included in the sliding window as the PBS score of the window. We kept the
206 sliding windows with an average PBS score in the 99th percentile and merged the top
207 sliding windows that are 10kb maximum from each other. The top PBS score of the
208 sliding windows in the region was given to the whole merged region.

209 In addition, we computed the cross-extended haplotype homozygosity (XP-EHH)⁴⁶ on
210 the phased dataset with selscan (v2.0.0)⁴⁷ to test for positive selection using haplotype
211 information (Note S12). We computed XP-EHH using PNG highlanders as the target
212 population and PNG lowlanders as the reference population. While the maximal scores
213 define regions under selection in PNG highlanders, the lowest scores indicate the

214 regions under selection in PNG lowlanders. We determined the top SNPs for XP-EHH
215 score in PNG highlanders as the SNP with XP-EHH score in the 99th percentile. We
216 kept the SNPs with XP-EHH score in the 1st percentile for PNG lowlanders. We
217 merged these top SNPs in windows: two top SNPs distant by at most 10kb are included
218 in the same window. This merging step results in windows whose endpoints are the
219 two most distant top SNPs included in the window.

220 Next, we combined the PBS and XP-EHH scores in a Fisher score⁴⁸ (Note S13). We
221 used the sliding windows of 20 SNPs, and 5 SNPs step defined for the PBS score. For
222 each of these sliding windows, we gave as XP-EHH score the highest XP-EHH score
223 among the 20 SNPs included in the windows. We combined the PBS and XP-EHH
224 scores in a Fisher Score $(-\log_{10}(PBS_{percentilrank}) - \log_{10}(XP - EHH_{percentilrank}))^{48}$ for
225 each sliding window. Finally, we selected the windows Fisher Score in the 99th
226 percentile and merged them when they were distant of maximum 10kb. We extended
227 the top 10 merged windows with the highest score for each of the three methods by a
228 50kb flanking region. Finally, we merged the overlapping regions from these 30 top
229 regions to obtain the final non-overlapping regions of interest that we will use further.

230 Because of the low number of individuals per population in the PNG diversity sets I
231 and II and the high genetic diversity in PNG (Figures S3-S4), we did not include these
232 samples in the selection analyses described above.

233 **Selection of the SNPs of interest**

234 We computed ancestral recombination graphs for the phased dataset with Relate
235 (v1.1.8)⁴⁹ (Note S14). We generated coalescence rates through time within PNG
236 highlanders and lowlanders from their respective subtrees. Finally, we extracted the
237 local tree for each SNP in the regions of interest from PNG highlanders and lowlander
238 subtrees. We used these local trees as input for Coalescent Likelihood Under Effects
239 of Selection (CLUES) (v1)⁵⁰ (Note S15). CLUES assigns a likelihood ratio (logLR) to
240 each SNP of interest that reflects the support for the non-neutral model. For each SNP
241 in the region of interest, we computed logLR five times by re-sampling the local tree
242 branch length and averaged the logLR for the five runs. To decide between the top five
243 SNPs with the higher average logLR in each genomic region, we generated the logLR
244 50 additional times for these five SNPs. We considered the SNP with the highest
245 average log LR after 50 runs as the SNP the most likely to drive selection within the
246 regions under selection (aka candidate SNPs). Because SNPs with low DAF (Derived

247 Allele Frequency) are unlikely to be under selection, we did not consider SNPs with
248 DAF lower than 5%. We also filtered out fixed variants for which CLUES cannot
249 compute the logLR.

250 **Association in the UK biobank**

251 To further understand how the candidate SNPs affect phenotypes, we downloaded the
252 UK biobank's summary statistics ⁵¹ for the 1,931 phenotypes with more than 10,000
253 samples (Note S17). We extracted the p-value and the beta of the candidate SNPs for
254 each phenotype. To avoid the ancestry sample size bias present in UKBB, we only
255 extracted the p-value (pval_EUR) and beta score (beta_EUR) for European ancestry.
256 Because the PNG population has a unique genetic diversity absent in Europeans,
257 some candidate SNPs were not listed in the UK biobank. In that case, we looked for
258 summary statistics for the closest SNP from a 1kb upstream and 1kb downstream
259 region. After extracting the SNP summary statistics for every phenotype, we only
260 consider the phenotype of interest if the log(p-value) is lower than -11.29 to correct for
261 multiple testing considering the significance threshold of $\log(10^{-8})$ that needs to be
262 corrected for the number of phenotypes studied ($\log_{10} \frac{10^{-8}}{1931}$). Finally, we corrected the
263 orientation of the beta value from the alternative allele to the derived allele.

264 **Association test**

265 We used Genome-wide Efficient Mixed Model Association (GEMMA) (v0.98.4) ⁵² to
266 detect if the candidate SNPs are associated with any phenotypes that we measured in
267 the PNG highlanders, lowlanders and PNG diversity set I datasets (Note S16). As we
268 did previously ¹⁵, we corrected the haemoglobin concentration, blood pressure, heart
269 rate and BMI for age and gender and the chest depth, waist circumference, weight,
270 and pulmonary function measurements (FEV1, PEF and FVC) for age, gender and
271 height using a multiple linear regression approach.

272 We performed association tests with a univariate Linear Mixed Model (LMM) for the
273 SNPs of interest and each corrected phenotype. To increase our sampling size, we
274 performed these association tests using all the PNG individuals (highlanders,
275 lowlanders and PNG diversity set I) with at least one phenotype measurement (n=234)
276 (Table S3). We incorporated into the LMM the centred relatedness matrix computed
277 with GEMMA using all the 234 PNG sequences to correct for population stratification.
278 We corrected each p-value for the number of SNPs tested with the Benjamini-
279 Hochberg procedure ^{53,54}. Because these phenotypes can be gathered in five groups

280 of highly correlated phenotypes ¹⁵, we used a threshold for significance of 0.01 (0.05/5)
281 to correct for the number of phenotypes tested.

282 **Introgression**

283 To reveal similarities between PNG haplotypes and archaic haplotypes for the genomic
284 regions under selection in PNG highlanders and lowlanders, we used haplostrips (v1.3)
285 ⁵⁵ within PNG, African, Asian and European samples with Altai ⁵⁶ Neanderthal or
286 Denisovan ⁵⁷ genome as reference haplotypes (Note S18). We explored archaic allele
287 frequencies in the Papuans from the SGDP dataset ³⁴ in the regions with introgressed
288 haplotypes in PNG highlanders and lowlanders. We calculated these frequencies on
289 aSNPs, which were defined to be SNPs with one allele (i) present in at least PNG high-
290 or lowlander, (ii) found in a homozygous state in one of the three archaics of the Altai,
291 Vindija Neanderthals and Denisovan ⁵⁶⁻⁵⁸ and (iii) being absent in the 1,000 Genomes
292 YRI population.

293 **Prediction of variant effect**

294 As an additional effort to decipher the function of the candidate SNPs (e.g. gene
295 expression or changes in protein sequence), we looked for significant eQTLs for each
296 candidate SNP using the Genotype-Tissue Expression (GTEx) Portal ⁵⁹. In addition,
297 we downloaded the 111 reference human epigenomes from the Roadmap
298 epigenomics project ⁶⁰ to explore which chromatin state the candidate SNPs fall in
299 different tissue types. Finally, we used The Ensembl Variant Effect Predictor (VEP) ⁶¹
300 on the region under selection to detect missense variants in these regions with the
301 canonical flag.

302 Results and discussion

303 Selection scans results in PNG highlanders and PNG lowlanders

304 To study selection specific to PNG highlanders or PNG lowlanders, we used 54 newly
305 sequenced genomes from three villages in PNG Highlands located in Mount Wilhelm
306 between 2,300 and 2,700 meters above sea level (a.s.l.) and 74 newly sequenced
307 genomes from Daru island (<100 m a.s.l.). We computed frequency-based (PBS) and
308 haplotype-based (XP-EHH) selection statistics – two selection tests based on distinct
309 genetic signatures – to detect candidate regions for selection in PNG highlanders and
310 lowlanders. Both selection statistics require a target and reference population, allowing
311 us to identify the signal of selection within the target population (PNG highlanders or
312 PNG lowlanders) but absent in the reference population (PNG lowlanders or PNG
313 highlanders, respectively). We also combined both these statistics in a Fisher Score ⁴⁸
314 to detect the region with extended haplotype homozygosity and carrying multiple
315 variants with high allele frequency. For each selection statistic (PBS, XP-EHH and
316 Fisher Score), we kept the ten regions with the highest score leading to 30 genomic
317 regions of interest for PNG highlanders and lowlanders (Tables S5-S6). We merged
318 the overlapping regions between methods, resulting in a final number of 21 regions of
319 interest in PNG highlanders (Tables 1, S5, Figure 1) and 23 in PNG lowlanders (Tables
320 2, S6, Figure 1).

321 The 21 regions showing signatures of selection in PNG highlanders encompass 54
322 genes, including genes involved in the regulation of platelet adhesion (ex: *FBLN1* ⁶²),
323 HIF-pathway (ex: *LINC02388* ⁶³), neurodevelopment (ex: *DLGAP1* ⁶⁴) and immunity
324 (ex: MHC locus ⁶⁵) (Tables 1, S5, Figure 1). The region with the highest Fisher score
325 and second highest PBS and XP-EHH scores in PNG highlanders includes the long
326 intergenic non-protein coding RNA *LINC02388*. This intergenic RNA is associated with
327 the serum levels of protein LRIG3 ⁶³ that impact angiogenesis – the formation of new
328 blood vessels – in glioma cells through regulation of the HIF-1 α /VEGF pathway ^{66,67}.
329 Comparably to other axes of the HIF pathway under selection in high-altitude
330 populations ^{9,10}, we hypothesise that this selection signature on *LINC02388* might
331 reflect adaptive processes counteracting hypoxia by affecting the formation of new
332 blood vessels. This axis of the HIF pathway might maintain oxygen transport to
333 appropriate levels in PNG highlanders while limiting the increase in haemoglobin
334 concentration and blood viscosity. Moreover, five of the ten regions with the highest

335 Fisher score include a gene associated with cardiovascular phenotypes (*FBLN1*⁶²,
336 *GLT8D2*⁶⁸, *DLGAP1*⁶⁹, *PTPRG*⁷⁰ and *SLC24A4*⁷¹). This observation supports our
337 hypothesis that selection in PNG highlanders acted on genes that might have helped
338 them to counteract the hypoxic condition of their environment.

339 Genomic selection candidate regions in PNG lowlanders encompassed multiple
340 immunity-related genes (*PLAC8*⁷², *SEC31A*⁷³, *PDCD1*⁷⁴, *DYNLL1*⁷⁵) (Tables 2, S6,
341 Figure 1). Notably, the region with the highest XP-EHH, PBS and Fisher Score includes
342 several genes from the guanine-binding protein family (GBP). This gene family is
343 associated with protective effects against diverse pathogens⁷⁶. The lowlander-specific
344 selection signature for this gene family, supports the hypothesis that adaptive
345 processes in this population were linked to the specific pathogenic pressure PNG
346 lowlanders faced.

347 **Selected SNPs phenotypic associations**

348 Next, we sought to identify the most likely selection target SNPs in each candidate
349 region. To this end we reconstructed allele frequency trajectories through time for all
350 the SNPs in a candidate region for selection for the last 980 generations (27,440
351 years), using CLUES⁵⁰ and selected the SNP with the largest average log(LR) (here
352 onwards they will be regarded as candidate SNPs; Tables 1-2, S7-S10). Next, we
353 applied two complementary approaches to explore the phenotypic effects of each
354 candidate SNPs. First, we queried GWAS summary statistics from the UK Biobank for
355 each candidate SNP. Seven candidate SNPs of PNG highlanders (or the closest SNPs
356 when the candidate SNP was not present in the UK Biobank) demonstrate significant
357 association with at least one phenotype of the UK Biobank (Table 1, Table S11-S12).
358 Three of these SNPs are significantly associated with haematological phenotypes.
359 Similarly, among PNG lowlanders, eight candidate SNPs show significant associations
360 in the UK Biobank and four with haematological phenotypes (Table 2, Table S13-S14).

361 We were able to replicate associations of these SNPs under selection and
362 cardiovascular components using phenotypes measurement done for PNG
363 highlanders, lowlanders and PNG diversity set I datasets. After correction for age,
364 gender and the number of tested SNPs, we identified two significantly associated
365 SNPs, both of which showed associations with heart rate ($p_{\text{val adjusted}} < 0.05$; p_{val}
366 adjusted for the number of SNPs tested) (Figure 2) although this association does not

367 survive after correcting the significance threshold for the number of tested phenotypes
368 ($p_{\text{val}_{\text{adjusted}}} > 0.01$) (Note S16, Table S15). The derived allele G of rs74576183-A/G, an
369 intronic variant of *NCAPD2*, that is under positive selection in PNG highlanders based
370 on CLUES results (Table S7) might be associated with a slower heart rate ($p_{\text{val}_{\text{adjusted}}} =$
371 0.046 , $\beta = -2.981$; Table S15, Figure 2). On the contrary, the derived allele T of
372 rs4693058-C/T, an intronic variant of *SEC31A*, that is under positive selection in PNG
373 lowlanders (Table S8) might be associated with a faster heart rate ($p_{\text{val}_{\text{adjusted}}} = 0.046$,
374 $\beta = 3.137$; Table S15, Figure 2). Interestingly, these two SNPs showed significant
375 associations with diverse haematological phenotypes in the UK biobank as well
376 (Tables S11, S13). It is possible that these associations with heart rate might reflect
377 an association with other haematological components that were not measured in the
378 PNG samples. Indeed, heart rate correlates with haematological components that are
379 usually overlooked and might be the real target of selection ¹⁴.

380 However, both the above-mentioned approaches have limitations. First, associations
381 from the UK biobank have been detected in a different population than Papuans; the
382 transferability of the directionality of the beta values of the associations is therefore
383 limited ⁷⁷. Secondly, we did not find any significant phenotype association for top
384 selection candidate SNPs when correcting for the number of SNPs and phenotypes
385 tested together. That may be because of the low sample size or the choice of
386 documented phenotypes that are not the direct target of selection. Nonetheless, the
387 associations in both analyses with related phenotypes support the hypothesis that
388 cardiovascular phenotypes were a target of selection within PNG highlanders and
389 lowlanders.

390 **Functional consequences of candidate SNPs**

391 In order to study the potential molecular effects and the most likely target genes of
392 selection candidate SNPs, we investigated their putative regulatory role and impact on
393 the protein structure. Five out of 21 candidate SNPs in PNG highlanders and three out
394 of 23 in PNG lowlanders – including SNPs rs74576183-A/G and rs4693058-C/T whose
395 derived alleles under selection are associated with heart-rate – show significant eQTLs
396 in various GTEx⁵⁹ tissues (Tables S16-S17). Furthermore, 17 out of the 21 putative
397 SNPs driving selection in PNG highlanders and 16 out of 23 in PNG lowlanders are in
398 moderate LD ($R^2 > 0.5$) with at least one variant with a predicted eQTL in the GETx
399 portal⁵⁹ (Tables S18, S19). Finally, 38 out of the 44 candidate SNPs overlapped with

400 open chromatin regions in at least one epigenome (Figures S5, S6). These results
401 suggest that some of the selection candidate SNPs play a role in gene expression in
402 various primary tissues and cell types.

403 In addition, we scanned top selected genomic regions for missense variants (Tables
404 S20, S21). We found 191 variants that alter the protein sequence of 18 genes among
405 PNG highlanders selected regions. Regions under selection in PNG lowlanders
406 encompass 85 missense variants that alter 21 genes. In PNG highlanders, one of the
407 regions under selection (chr12:6502552-6612260) overlaps with one missense variant
408 (TAPBPL-G151V), a variant with an exceptionally high derived allele frequency (DAF)
409 in PNG highlanders (DAF = 0.7, <12% in African, Asian or European populations; Table
410 S20). Moreover, this missense variant is in high LD ($R^2=0.952297$) with the candidate
411 SNP, rs74576183-A/G. In contrast, the selection candidate region encompassing GBP
412 overlaps with a missense variant (GBP2-A549P) which is absent in non-Papuan
413 populations and a DAF of 82% in PNG lowlanders (Table S21). This variant is in
414 moderate LD ($R^2=0.57$) with the candidate SNP for the region (rs368120563-T/C).
415 While we expect CLUES top results to be enriched for the causal SNPs of selection, it
416 remains possible that the real targets of selection are SNPs linked to our candidate
417 SNPs. In the case of rs368120563-T/C, we suggest that the linked missense variant
418 GBP2-A549P modifying protein sequence might be the real target of selection for the
419 genomic region.

420 **Archaic introgressions in loci under selection**

421 We used haplostrips⁵⁵ to scan regions with selection signatures in PNG highlanders
422 or PNG lowlanders for archaic haplotypes. We observed ten such regions in PNG
423 highlanders (Tables 1, S22). Five of these regions contain archaic SNPs with allele
424 frequencies that are located within the top 10% in Papuans from the SGDP dataset
425 (Table S22). The region with the highest XP-EHH, PBS and Fisher score and carrying
426 *LINC02388* – that might regulate angiogenesis through the HIF/VEGF pathway –
427 carries an archaic haplotype that shows high sequence similarity with the Altai
428 Neanderthal. Rs74576183-A/G, the SNP whose derived allele was under selection in PNG
429 highlanders is associated with a slower heart rate, is located in a region carrying a
430 Denisovan-like haplotype (Figure S10).

431 Within regions under selection in PNG lowlanders, we observed six regions with
432 evidence for archaic introgression (Tables 2, S23). Among these is the region
433 encompassing the immunity-related GBP locus (Figure 3) which exhibits the highest
434 selection peak in PNG lowlanders and shows haplotypes with sequence similarities to
435 both Denisovan and Altai Neanderthal. Archaic introgression in this region has
436 previously been reported in Melanesians^{31,35}. But interestingly, the sequence of the
437 introgressed haplotypes does not match with either Vindija⁵⁸ or Chagyrskaya⁷⁸
438 Neanderthals (data not shown). These two Neanderthals are a better reference for the
439 introgressed Neanderthal population in non-African populations than Altai Neanderthal
440⁵⁸. This fact and the gene flow between the Altai Neanderthal and Denisova⁵⁷ would
441 suggest that we most likely observed Denisovan introgression within the GBP locus in
442 the PNG population.

443 Finally, two candidate SNPs for each studied PNG population (total four SNPs) are
444 exclusively found on introgressed haplotypes (Figure 3, S7-S9) and absent on non-
445 archaic haplotypes. Since these SNPs are not fixed on the archaic haplotypes, this
446 pattern would suggest that the selected mutation appeared after the introgression
447 event and selection of the mutation led to an increase of the introgressed haplotype.
448 Another scenario is that Neanderthal and/or Denisovans were variable at this genomic
449 position and introgressed haplotypes with and without the variant and that both types
450 of haplotypes are still segregating in present-day Papuans.

451 **Cardio Vascular, a target for selection in PNG highlanders**

452 In summary, our analysis of selective pressures in Papuan highlanders suggest that
453 top selected regions encompass genes that might have contributed to counteracting
454 hypoxia detrimental effect in PNG highlanders and that candidate selection SNPs show
455 associations with blood-related phenotypes. For example, the genomic regions on
456 chr12 overlapping with the gene *NCAPD2* demonstrates how hypoxic pressure may
457 have impacted the genome and phenotypes of PNG highlanders. This region shows
458 the third-highest XP-EHH score in PNG highlanders (Table 1, Figure 1). The candidate
459 SNP for this region, rs74576183-A/G (Figure 2), overlaps with the gene *NCAPD2* that
460 is involved in various neurodevelopmental disorders^{79–82}. Similarly, genomic regions
461 under selection in Andeans living at intermediate altitude show enrichment for
462 neuronal-related genes, which might protect their brain from hypoxic damage⁸³.
463 Indeed, hypoxia at altitude impacts brain development and function when exposed

464 during perinatal life^{84,85} or long after birth^{86,87}. This candidate SNP derived allele under
465 selection shows a significant association with increasing red blood cell count in the UK
466 Biobank (Table S11), and for association with slower heart rate from phenotypes
467 measured in PNG (Figure 2, Table S15) supports adaptation through some
468 cardiovascular related process. The fact that this SNP shows significant eQTL
469 associations and overlaps with open chromatin state in multiple tissues would supports
470 its role in gene expression regulation. However, because this SNPs is in high LD with
471 a missense variant with high DAF in PNG Highlanders but rare in other populations
472 (Table S20), it is also possible that the real target for selection might be the missense
473 variant (TAPBPL-G151V) that leads to changes in the TAPBPL protein that is
474 associated with antigen processing. This region under selection overlap with
475 Denisovan-like archaic haplotypes (Tables 1, S22, Figure S10) but neither the
476 candidate SNP nor the missense variant derived allele are found in PNG individuals
477 that carry this archaic haplotype (Figure S10).

478 **Immunity, a target for selection in PNG lowlanders**

479 Similarly, the region containing the gene *SEC31A* and rs4693058-C/T, the candidate
480 SNP for this region (Figure 2), are of particular interest to selection for pathogenic
481 pressure in PNG lowlanders. Indeed *SEC31A*⁷³ might play a role in immune
482 processes, and the derived allele under selection of rs4693058-C/T, the candidate
483 SNP for this locus, shows a significant association with various white cells percentages
484 and counts (Table S13). Interestingly derived allele T under selection of rs4693058-
485 C/T shows a suggestive association with faster heart rate (Figure 2). But once again,
486 we suggest that heart rate might be a proxy for other phenotypes (here the white cells
487 count⁸⁸). Because rs4693058-C/T show significant eQTLs and overlaps with open
488 chromatin states in multiple tissues (Table S17, Figure S6), we hypothesise that it
489 impacts gene expression regulation. This region under selection overlaps with an
490 introgressed haplotype from Denisovan, but the introgressed haplotype does not carry
491 the derived allele of the candidate SNP (Figure S11).

492 Finally, the regions with the highest XP-EHH, PBS and Fisher Score in PNG lowlanders
493 (Figure 1, Tables 2, S6), includes several genes from the guanine-binding protein
494 (GBP) associated with immunity to diverse pathogens⁷⁶. Especially, Apinjuh et al.
495 reported an association between *GBP7* variant and higher malaria symptoms in the
496 Cameroon population⁸⁹, suggesting this region might be selected due to malaria. The

497 candidate SNP, rs368120563-T/C, is in LD with a missense variant (GBP2-A549P)
498 with a high DAF in PNG lowlanders (DAF=0.82) but absent in non-Papuan populations
499 (Table S21). This missense variant is part of the top 5 SNPs given by CLUES for the
500 region (Table S10). That might suggest that we failed to identify the real selection
501 driving SNP when limiting the candidate SNPs to the first top one. This particular
502 missense variant might be the causal SNP and selection might have targeted a change
503 in the GBP2 protein sequence. This GBP locus carries a Denisovan-like haplotype that
504 includes both the candidate variant of the region (rs368120563-T/C) and the missense
505 variant (GBP2-A549P) in PNG populations. Moreover, the missense variant can be
506 found in the Denisovan genome, but the candidate SNP is not present in the Denisovan
507 or any of the high coverage Neandertal genomes (Figure 3). That pattern is compatible
508 with the scenario where the candidate variant appeared after the introgression and that
509 the introgressed haplotype frequency increased in the PNG populations driven by the
510 selection acting on this variant. The alternative hypothesis would be that the candidate
511 variant is not the target of selection (most likely the missense variant is), and the
512 candidate variant is hitchhiked with the selected and introgressed haplotype.

513 Conclusion

514 In this paper we investigated selection in PNG highlanders and PNG lowlanders and
515 detected 21 and 23 genomic regions under positive selection, respectively. Within each
516 candidate selection region, we identified the SNP that most likely drives selection and
517 explore their association with several phenotypes measured within our dataset or UK
518 Biobank summary statistics. The genes in regions that show selection signals in PNG
519 highlanders are associated with HIF pathway regulation, brain development, blood
520 composition and immunity. PNG lowlanders show selection for immune system. In both
521 populations, one of the candidate SNPs suggests an association with heart rate. This
522 SNP and several top SNPs were also significantly associated with several blood
523 composition phenotypes in the UK Biobank. Further studies will be needed to clarify
524 the complexity of the PNG's haematological responses to hypoxia and pathogenic
525 pressures. We found that 16 regions under selection -10 in PNG highlanders and 6 in
526 PNG lowlanders – carry archaic introgression. Out of which, two candidate SNPs from
527 both populations (a total of four) reside directly inside the introgressed haplotypes
528 suggesting adaptive introgression. Our results suggest that selection in PNG
529 highlanders and lowlanders was partially targetting introgressed haplotypes from

530 Neandertals and Denisovans. This study demonstrates that both PNG highlanders and
531 PNG lowlanders carry signatures of positive selection and that the associated
532 phenotypes largely match with the challenges they faced due to the environmental
533 differences.

534 Authors contribution

535 F.-X.R., N.B., M.L., T.O. and M.Me. designed the study. F.-X.R, N.B., M.L., J.K., N.E.
536 and J.M. collected the data. V.M., A.B., and J.F.D. generated whole-genome
537 sequences. M.A., N.B., G.H., V.P., D.Y., R.K. and M.Mo. performed the data analysis.
538 F.-X.R., M.Me. and M.P.C. provided resources and logistics. M.A., N.B., M.Mo. and F-
539 X.R. wrote the manuscript with the contribution from all the co-authors.

540 Data availability

541 PNG highlanders (n=38) and lowlanders (n=46) sequenced genomes are on the
542 European Genome-Phenome data repository: EGAXXX.

543 Funding

544 M.A. was supported by the European Union through the European Regional
545 Development Fund (Project No. 2014-2020.4.01.16-0030). , G.H., V.P., R.K., M.D.,
546 T.O. and M.Mo. were supported by the European Union through Horizon 2020
547 research and innovation programme under grant no 810645 and the European
548 Regional Development Fund project no. MOBEC008. This work was supported by the
549 French Ministry of Foreign and European Affairs (<https://www.diplomatie.gouv.fr>)
550 (French Prehistoric Mission in Papua New Guinea to F.-X.R.), the French Embassy in
551 Papua New Guinea (<https://pg.ambafrance.org>), and the University of Papua New
552 Guinea, Archaeology Laboratory Group. We acknowledge support from the LabEx
553 TULIP, France (<https://www.labex-tulip.fr>) (to F.-X. R. and N. B.) and the French
554 Ministry of Research grant Agence Nationale de la Recherche (<https://anr.fr>) number
555 ANR-20-CE12-0003-01 (to F.-X.R.); from the Leakey Foundation
556 (<https://leakeyfoundation.org>) (to N. B.). The CNRGH sequencing platform was
557 supported by the “France Génomique” national infrastructure, funded as part of the
558 “Investissements d’Avenir” program managed by the “Agence Nationale pour la
559 Recherche” (contract ANR-10-INBS-09).

560 Acknowledgments

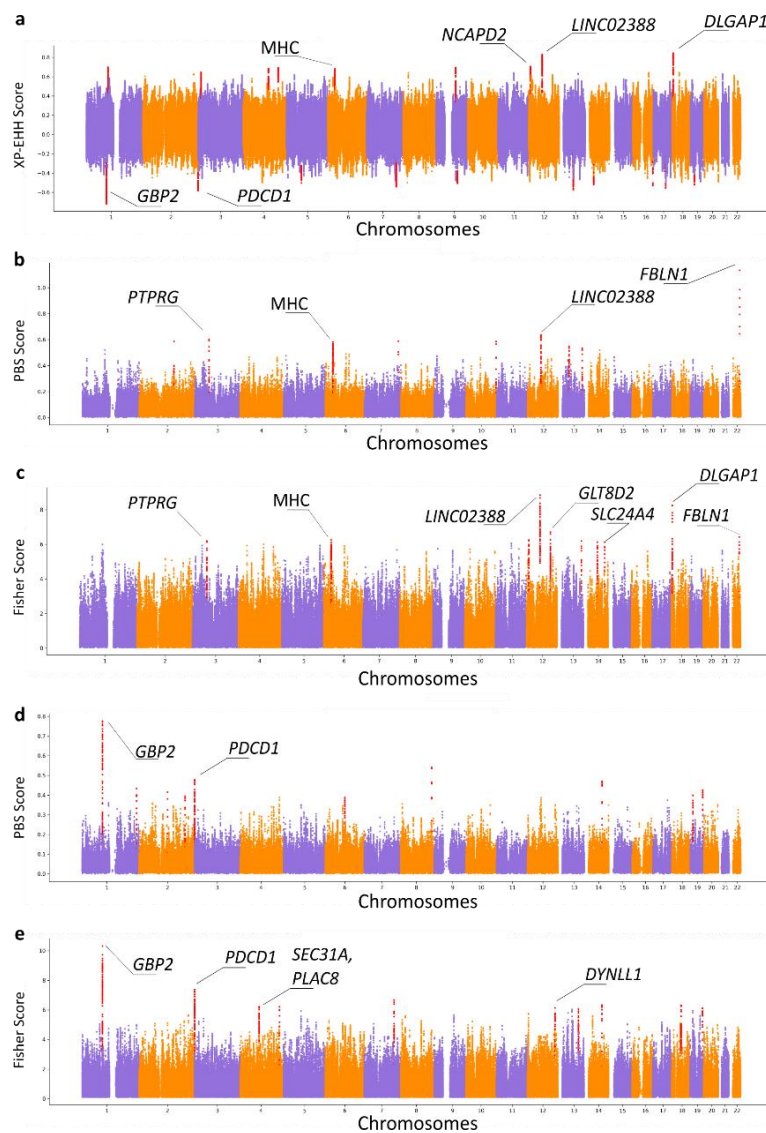
561 We kindly thank F.-X. Ricaut for giving us access to additional PNG whole genome
562 sequences from Daru, Mt. Wilhelm and Port Moresby. These data were generated at
563 the National Center of Human Genomics Research (France) or the KCCG Sequencing

564 Laboratory (Garvan Institute of Medical Research, Australia). We thank Ray Tobler
565 (Australian National University), Roxanne Tsang (Centre for Social and Cultural
566 Research, Griffith University, Australia), Kylie Sesuki and Teppsy Beni (School of
567 Humanities and Social Sciences, University of Papua New Guinea), and Alois Kuaso
568 and Kenneth Miamba (National Museum and Art Gallery, Papua New Guinea) for their
569 help during the sampling campaigns. We especially thank all of our study participants.
570 Data analyses were carried out in part in the High-Performance Computing Center of
571 the University of Tartu.

572 **Competing interest**

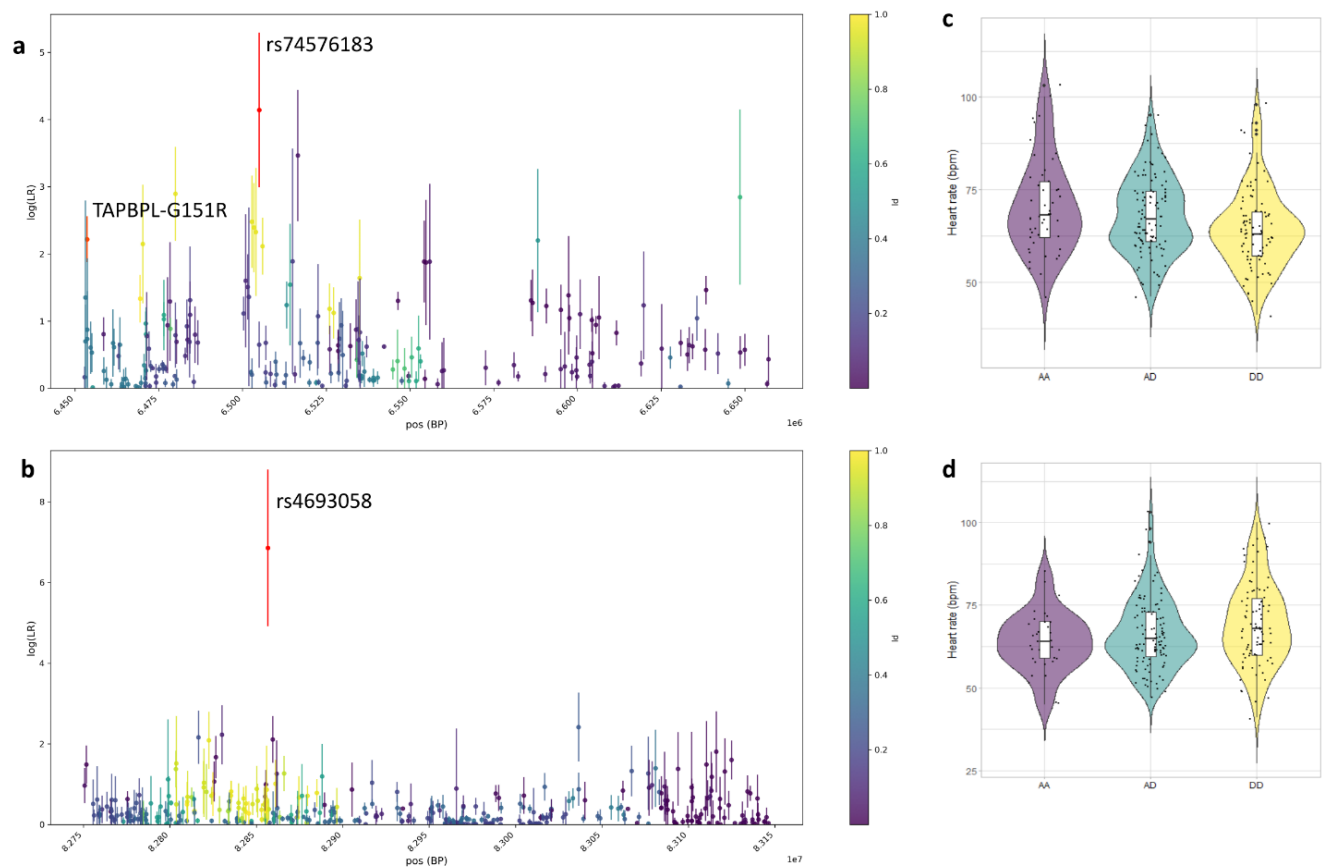
573 The authors declare no competing interest.

574



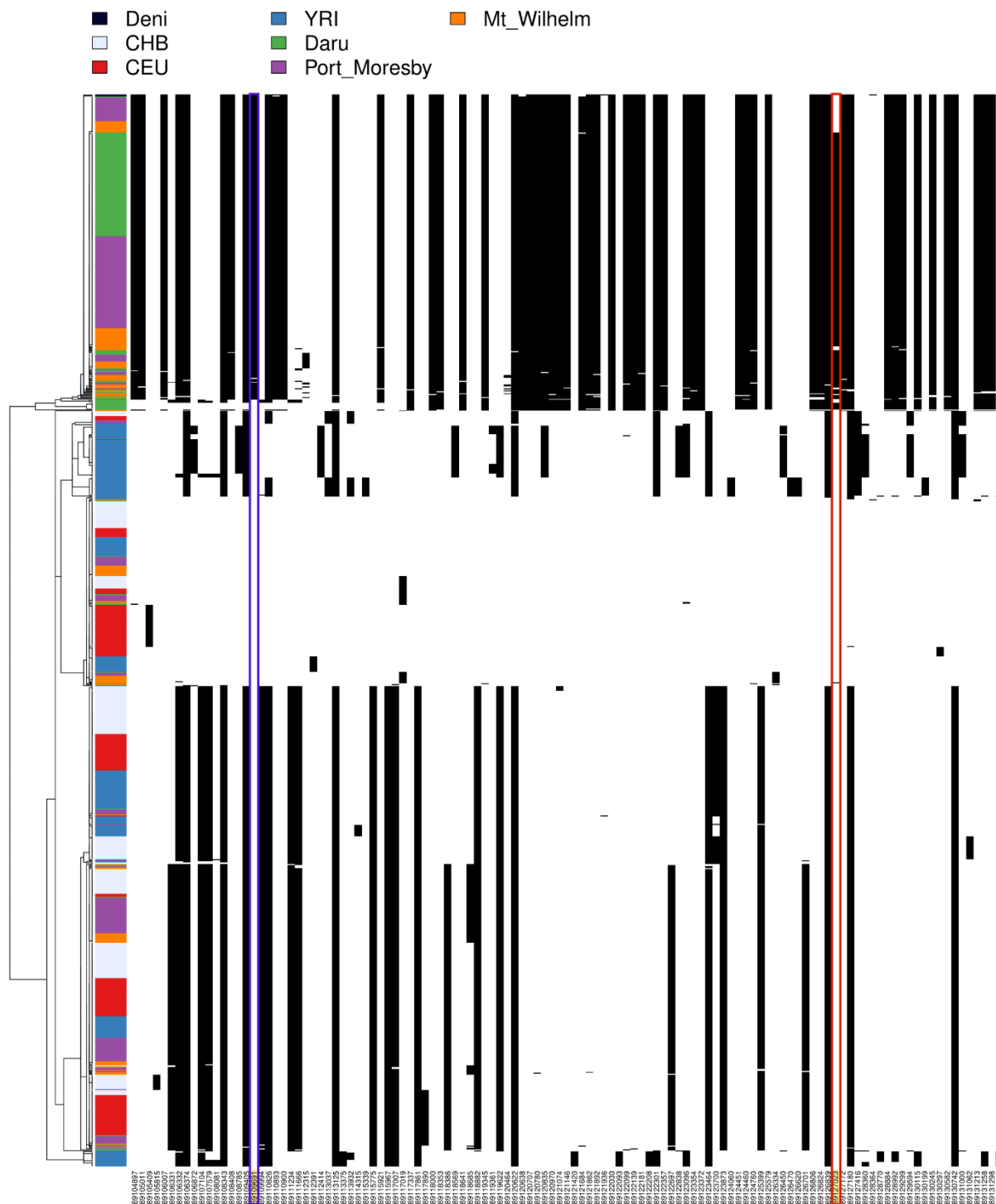
575

576 **Figure 1: Manhattan plots for the three selection scans among PNG highlanders**
577 **and lowlanders.** Candidate genes discussed in the paper are shown. **(a)** XP-EHH
578 scores using PNG highlanders as the target population and PNG lowlanders as the
579 reference population. Genomic regions with the highest score indicate selection in
580 PNG highlanders. Genomic regions with the lowest score indicate selection in PNG
581 lowlanders. **(b)** PBS scores using PNG highlanders as the target population, PNG
582 lowlanders as the reference population, and Yorubas from 1000G as the outgroup. **(c)**
583 Fisher Scores combining the PBS and XP-EHH scores of PNG highlanders. **(d)** PBS
584 scores using PNG lowlanders as the target population, PNG highlanders as the
585 reference population, and Yorubas from 1000G as the outgroup. **(e)** Fisher Scores
586 combining the PBS and XP-EHH scores of PNG lowlanders.



587

588 **Figure 2: a, b $\log(\text{LR})$ for SNPs in regions under selection** after 5 runs of CLUES
589 or 50 runs of CLUES for each of the five top SNPs for the candidate region. Candidate
590 SNP driving selection for the region are shown in red. Colour scale indicates linkage
591 disequilibrium with the candidate SNP. (a) Region chr12:6452552-6662260, that is
592 under selection in PNG highlanders. Candidate SNP for the region is rs74576183-A/G.
593 Missense variant (TAPBPL-G151V) in high LD with rs74576183-A/G is shown in
594 orange. (b) Region chr4:82750503-83146792, that is under selection in PNG
595 lowlanders. Candidate SNP is rs4693058-C/T. **c, d Violin plot of the heart rate**
596 **distribution in PNG depending of their genotype for the candidate SNPs** (A =
597 ancestral allele, D = derived allele (under selection)) (c) rs7457618-A/G, AA=AA,
598 AD=AG, DD=GG(d) and rs4693058-C/T, AA=CC, AD=CT, DD=TT.



599

600

601

602

603

604

605

606

Figure 3: Haplotrips plot for the region chr1:88800562-89326878 overlapping with the GBP locus and under selection in PNG lowlanders. Introgression from Altai Denisovans in PNG for in this region. Derived alleles are plotted in black and ancestral are in white. The introgressed haplotype carry the SNP driving selection for the region (rs368120563-T/C, framed in orange) but the Altai Denisova does not have this particular allele. On the contrary, the missense variant (framed in blue) in LD with rs36812056 is found in the introgressed haplotype and in Denisovan genome

607 **Table 2: Merged regions under selection and SNP most likely to be selected in PNG highlanders**

Merged top regions	Score	Protein coding genes in the region	Archaic introgression	Candidate SNP for the region	DAF	Significant association (UK Biobank)	Distance to the closest SNP in UKBB (BP)
chr1:95529290-95736826	XPEHH	.	Denisova	rs887476833-G/A	0.55	-*	+ 33
chr2:151012094-151201575	PBS	.	.	rs74621527-G/A	0.92	-	0
chr3:13010340-13217789	XPEHH	IQSEC1	Denisova	rs374181005-T/C	0.41	-*	- 50
chr3:61779523-62009858	PBS, Fisher	PTPRG	.	rs79600167-G/A	0.77	-	0
chr4:110182324-110384099	XPEHH	ELOVL6	Altai Neanderthal	rs943845085-G/A	0.42	-*	- 22
chr4:152704503-152970509	XPEHH	<i>TIGD4, ARFIP1, FHDC1</i>	.	rs369030953-A/G	0.59	-	- 88
chr6:30916070-31153184†	XPEHH	<i>VARS2, SFTA2, MUCL3, MUC21, MUC22, HCG22, C6orf5, PSORS1C1, CDSN, PSORS1C2, PSORS1C1, CCHCR1</i>	.	rs940110341-G/A	0.61	Blood composition* (Table S12)	+ 94
chr6:33006055-33132312†	PBS, Fisher	<i>HLA-DAO, HLA-DPA1, HLA-DPB2</i>	.	rs9277772-T/C	0.21	Body proportion, blood composition, other phenotypes (Table S11)	0
chr7:147590904-147718219	PBS	CNTNAP2	.	rs17170618-T/C	0.52	-	0
chr9:85458922-85745092	XPEHH	AGTPBP1	.	rs28728004-C/A	0.69	Other phenotypes* (Table S12)	- 7
chr10:131112245-131235951	PBS	TCERG1L	Altai Neanderthal	rs10829909-T/G	0.43	-	0
chr12:6452552-6662260	XPEHH	<i>TAPBPL, VAMP1, MRPL51, GAPDH, NOP2, LPAR5, ING4, ACRBP, CHD4, IFFO1, NCAPD2</i>	Denisova	rs74576183-A/G	0.71	Blood composition (Table S11)	0
chr12:9886812-10055333	Fisher	<i>KLRF2, CLEC2A, CLEC12A, CLEC1B, CLEC12B, CLEC9A</i>	.	rs536947-C/T	0.91	-	0
chr12:58391529-58634980	XPEHH, PBS, Fis	.	Altai Neanderthal	rs376870800-A/G	0.70	-*	- 160
chr12:103783315-104121479	Fisher	NT5DC3, HSP90B1, GLT8D2, HCFC2, NFYB, TDG	Denisova	rs1032698711-G/A	0.47	-*	- 22
chr13:47639988-47825193	PBS	.	.	rs1033760372-C/A	0.19	-*	- 34
chr13:104734734-104875020	PBS, Fisher	.	Denisova	rs16965509-G/A	0.50	-	0
chr14:60157772-60377317	Fisher	PCNX4, DHRS7, PPM1A	Denisova	rs1033848215-A/G	0.32	Other phenotypes* (Table S12)	- 2
chr14:92230479-92401520	Fisher	SLC24A4	.	rs8003454-C/T	0.52	-	0
chr18:4072997-4251153	XPEHH, Fisher	DLGAP1	Altai Neanderthal	rs371858795-G/A	0.77	Other phenotypes* (Table S12)	+ 124
chr22:45519818-45644906	PBS, Fisher	FBLN1	.	rs1601558750-G/A	0.10	Body proportion* (Table S12)	+ 101

608

609 Genomic coordinates are given for GRCh38

610 DAF is given for PNG lowlanders.

611 †Reference Assembly Alternate Haplotype Sequence Alignments

612 *SNP not present in the UK Biobank, we look association for the closest SNP within 1KB upstream and downstream region

613 Genes in bold are the closest to the candidate SNP defined with CLUES for the region

614 Putative introgressed regions are given using haplostrips

615 **Table 2: Merged regions under selection and SNP most likely to be selected in PNG lowlanders**

Merged top regions	Score	Protein coding genes in the region	Archaic introgression	Candidate SNP for the region	DAF	Significant association (UK Biobank)	Distance to the closest SNP in UKBB (BP)
chr1:88800562-89326878	XPEHH, PBS, Fisher	<i>PKN2, GTF2B, KYAT3, RBMXL1, GBP3, GBP1, GBP2, GBP7, GBP4, GBP5</i>	Denisova Altai Neanderthal	rs368120563-T/C	0.87	.*	+ 123
chr1:237827847-237992467	PBS	<i>RYR2, ZP4</i>	.	rs1574154373-G/A	0.14	.*	+ 36
chr2:124085628-124249405	PBS	CNTNAP5	.	rs7583123-G/T	0.49	-	0
chr2:200238798-200432145	PBS	SPATS2L	.	chr2:200269472-A/G	0.05	.*	+ 7
chr2:241759136-242088831†	XPEHH, PBS, Fisher	<i>GAL3ST2, NEU4, PDCD1, RTP5, FAM240C</i>	Altai Neanderthal	rs376150658-G/A	0.23	.*	+ 8
chr4:82750503-83146792	Fisher	<i>SCD5, SEC31A, LIN54, COPS4, PLAC8</i>	Denisova	rs4693058-C/T	0.76	Blood composition (Table S13)	0
chr4:171791098-171986729	Fisher	GALNTL6	.	rs926184421-G/A	0.08	Other phenotypes* (Table S14)	+ 14
chr5:65504470-65708617	XPEHH	<i>CENPK, TRIM23, SGTB, PPWD1, SHLD3, TRAPPC13</i>	.	rs36003688-T/C	0.31	-	0
chr6:85266477-85483888	PBS	NT5E	.	rs989789809-T/C	0.14	.*	+ 13
chr7:129548370-129836070	XPEHH, Fisher	<i>NRF1, UBE2H</i>	Denisova	rs6950082-T/A	0.49	Blood composition, other phenotypes* (Table S14)	+ 3
chr8:133791891-133962825	PBS	.	.	rs187915256-C/T	0.99	.*	+ 1
chr9:93717217-93877803	XPEHH	.	.	rs372277219-G/T	0.22	Other phenotypes* (Table S14)	+ 143
chr12:120353731-120666335	Fisher	<i>MSI1, COX6A1, GATC, TRIAP1, SRSF9, DYNLL1, COQ5, RNF10, POP5, CABP1</i>	.	rs75047318-T/C	0.07	Blood composition, body proportion, respiratory capacities, other phenotypes (Table S13)	0
chr13:61590770-61993327	XPEHH	.	.	rs537391125-A/G	0.94	Other phenotypes* (Table S14)	+ 81
chr13:89660867-89920623†	Fisher	.	.	rs72634302-G/A	0.48	-	0
chr14:37137933-37382802	XPEHH	<i>SLC25A21, MIPOL1</i>	.	rs1594377001-C/T	0.05	.*	+ 27
chr14:77312867-77558267	PBS, Fisher	<i>POMT2, GSTZ1, SAMD15, NOXRED1, VIPAS39, ISM2, SPTLC2, TMED8, AHS1</i>	.	rs12885954-C/T	0.57	-	0
chr16:87806834-87928392	XPEHH	<i>SLC7A5, CA5A</i>	.	rs2287123-G/A	0.32	Other phenotypes (Table S13)	0
chr17:54003406-54222843	XPEHH	.	Denisova	rs575590765-T/C	0.11	.*	+ 78
chr18:41133289-41618597	Fisher	.	.	rs2848745-G/C	0.95	-	0
chr19:11708670-12108034	PBS	<i>ZNF823, ZNF441, ZNF491, ZNF440, ZNF439, ZNF69, ZNF700, ZNF763, ZNF433, ZNF20, ZNF878, ZNF844</i>	Altai Neanderthal	rs900717974-C/T	0.11	.*	+ 32
chr19:16344294-16576199	XPEHH	<i>EPS15L1, CALR3, CHERP, C19orf44, SLC35E1, MED26</i>	.	rs1870071-C/T	0.76	Blood composition (Table S13)	0
chr19:54176104-54330609†	PBS, Fisher	<i>MBOAT7, TSEN34, RPS9, LILRB3, LILRA6, LILRB5, LILRB2, LILRA5</i>	.	rs1600734199-A/T	0.13	.*	+ 90

616

617 Genomic coordinates are given for GRCh38

618 DAF is given for PNG lowlanders.

619 †Reference Assembly Alternate Haplotype Sequence Alignments

620 *SNP not present in the UK Biobank, we look association for the closest SNP within 1KB upstream and downstream region

621 Genes in bold are the closest to the candidate SNP defined with CLUES for the region

622 Putative introgressed regions are given using haplostrips

623 References

- 624 1. Clarkson, C. *et al.* Human occupation of northern Australia by 65,000 years ago. *Nature* **547**,
625 306–310 (2017).
- 626 2. O’Connell, J. F. *et al.* When did Homo sapiens first reach Southeast Asia and Sahul? *PNAS* **115**,
627 8482–8490 (2018).
- 628 3. Brucato, N. *et al.* Papua New Guinean Genomes Reveal the Complex Settlement of North Sahul.
629 *Molecular Biology and Evolution* (2021) doi:10.1093/molbev/msab238.
- 630 4. Summerhayes, G. R., Field, J. H., Shaw, B. & Gaffney, D. The archaeology of forest exploitation
631 and change in the tropics during the Pleistocene: The case of Northern Sahul (Pleistocene New
632 Guinea). *Quaternary International* **448**, 14–30 (2017).
- 633 5. Brookfield, H. & Allen, B. High-Altitude Occupation and Environment. *Mountain Research and*
634 *Development* **9**, 201–209 (1989).
- 635 6. Müller, I., Bockarie, M., Alpers, M. & Smith, T. The epidemiology of malaria in Papua New
636 Guinea. *Trends in Parasitology* **19**, 253–259 (2003).
- 637 7. Trájer, A. J., Sebestyén, V. & Domokos, E. The potential impacts of climate factors and malaria on
638 the Middle Palaeolithic population patterns of ancient humans. *Quaternary International* **565**,
639 94–108 (2020).
- 640 8. Beall, C. M. Adaptation to High Altitude: Phenotypes and Genotypes. *Annu. Rev. Anthropol.* **43**,
641 251–272 (2014).
- 642 9. Moore, L. G. Human genetic adaptation to high altitudes: Current status and future prospects.
643 *Quat. Int.* **461**, 4–13 (2017).
- 644 10. Bigham, A. W. & Lee, F. S. Human high-altitude adaptation: forward genetics meets the HIF
645 pathway. *Genes Dev.* **28**, 2189–2204 (2014).
- 646 11. Lee, P., Chandel, N. S. & Simon, M. C. Cellular adaptation to hypoxia through hypoxia inducible
647 factors and beyond. *Nat Rev Mol Cell Biol* **21**, 268–283 (2020).

- 648 12. Beall, C. M. *et al.* Hemoglobin concentration of high-altitude Tibetans and Bolivian Aymara.
649 *American Journal of Physical Anthropology* **106**, 385–400 (1998).
- 650 13. Villafuerte, F. C. & Corante, N. Chronic Mountain Sickness: Clinical Aspects, Etiology,
651 Management, and Treatment. *High Alt Med Biol* **17**, 61–69 (2016).
- 652 14. Stemberge, M. *et al.* The overlooked significance of plasma volume for successful adaptation to
653 high altitude in Sherpa and Andean natives. *Proc Natl Acad Sci U S A* **116**, 16177–16179 (2019).
- 654 15. André, M. *et al.* Phenotypic differences between highlanders and lowlanders in Papua New
655 Guinea. *PLOS ONE* **16**, e0253921 (2021).
- 656 16. Moore, L. G. Measuring high-altitude adaptation. *Journal of Applied Physiology* **123**, 1371–1385
657 (2017).
- 658 17. Xue, B. & Leibler, S. Benefits of phenotypic plasticity for population growth in varying
659 environments. *Proceedings of the National Academy of Sciences* **115**, 12745–12750 (2018).
- 660 18. GBD 2013 Mortality and Causes of Death Collaborators. Global, regional, and national age–sex
661 specific all-cause and cause-specific mortality for 240 causes of death, 1990–2013: a systematic
662 analysis for the Global Burden of Disease Study 2013. *The Lancet* **385**, 117–171 (2015).
- 663 19. Kitur, U., Adair, T., Riley, I. & Lopez, A. D. Estimating the pattern of causes of death in Papua New
664 Guinea. *BMC Public Health* **19**, 1322 (2019).
- 665 20. Naraqi, S., Feling, B. & Leeder, S. R. Disease and death in Papua New Guinea. *Medical Journal of*
666 *Australia* **178**, 7–8 (2003).
- 667 21. World Health Organization. *World malaria report 2021*. (World Health Organization, 2021).
- 668 22. Senn, N. *et al.* Population Hemoglobin Mean and Anemia Prevalence in Papua New Guinea: New
669 Metrics for Defining Malaria Endemicity? *PLOS ONE* **5**, e9375 (2010).
- 670 23. Riley, I. D. Population change and distribution in Papua New Guinea: an epidemiological
671 approach. *Journal of Human Evolution* **12**, 125–132 (1983).
- 672 24. Trájer, A. J. Late Quaternary changes in malaria-free areas in Papua New Guinea and the future
673 perspectives. *Quaternary International* (2022) doi:10.1016/j.quaint.2022.04.003.

- 674 25. Reich, D. *et al.* Genetic history of an archaic hominin group from Denisova Cave in Siberia. *Nature*
675 **468**, 1053–1060 (2010).
- 676 26. Larena, M. *et al.* Philippine Aytas possess the highest level of Denisovan ancestry in the world.
677 *Curr Biol* S0960-9822(21)00977-5 (2021) doi:10.1016/j.cub.2021.07.022.
- 678 27. Huerta-Sánchez, E. *et al.* Genetic Signatures Reveal High-Altitude Adaptation in a Set of Ethiopian
679 Populations. *Mol Biol Evol* **30**, 1877–1888 (2013).
- 680 28. Vespasiani, D. M. *et al.* Denisovan introgression has shaped the immune system of present-day
681 Papuans. *PLOS Genetics* **18**, e1010470 (2022).
- 682 29. Choin, J. *et al.* Genomic insights into population history and biological adaptation in Oceania.
683 *Nature* 1–7 (2021) doi:10.1038/s41586-021-03236-5.
- 684 30. Jacobs, G. S. *et al.* Multiple Deeply Divergent Denisovan Ancestries in Papuans. *Cell* **177**, 1010-
685 1021.e32 (2019).
- 686 31. Brucato, N. *et al.* Chronology of natural selection in Oceanian genomes. *iScience* 104583 (2022)
687 doi:10.1016/j.isci.2022.104583.
- 688 32. Bergström, A. *et al.* Insights into human genetic variation and population history from 929
689 diverse genomes. *Science* **367**, (2020).
- 690 33. Malaspina, A.-S. *et al.* A genomic history of Aboriginal Australia. *Nature* **538**, 207–214 (2016).
- 691 34. Mallick, S. *et al.* The Simons Genome Diversity Project: 300 genomes from 142 diverse
692 populations. *Nature* **538**, 201–206 (2016).
- 693 35. Vernot, B. *et al.* Excavating Neandertal and Denisovan DNA from the genomes of Melanesian
694 individuals. *Science* **352**, 235–239 (2016).
- 695 36. The 1000 Genomes Project Consortium *et al.* A global reference for human genetic variation.
696 *Nature* **526**, 68–74 (2015).
- 697 37. Chen, S., Zhou, Y., Chen, Y. & Gu, J. fastp: an ultra-fast all-in-one FASTQ preprocessor.
698 *Bioinformatics* **34**, i884–i890 (2018).
- 699 38. broadinstitute/picard. (2022).

- 700 39. Poplin, R. *et al.* Scaling accurate genetic variant discovery to tens of thousands of samples.
701 201178 Preprint at <https://doi.org/10.1101/201178> (2018).
- 702 40. Auwera, G. van der & O'Connor, B. D. *Genomics in the cloud: using Docker, GATK, and WDL in*
703 *Terra*. (O'Reilly Media, 2020).
- 704 41. Patterson, N., Price, A. L. & Reich, D. Population Structure and Eigenanalysis. *PLOS Genetics* **2**,
705 e190 (2006).
- 706 42. Purcell, S. *et al.* PLINK: A Tool Set for Whole-Genome Association and Population-Based Linkage
707 Analyses. *Am J Hum Genet* **81**, 559–575 (2007).
- 708 43. Alexander, D. H., Novembre, J. & Lange, K. Fast model-based estimation of ancestry in unrelated
709 individuals. *Genome Res* **19**, 1655–1664 (2009).
- 710 44. Delaneau, O., Zagury, J.-F., Robinson, M. R., Marchini, J. L. & Dermitzakis, E. T. Accurate, scalable
711 and integrative haplotype estimation. *Nature Communications* **10**, 5436 (2019).
- 712 45. Yi, X. *et al.* Sequencing of 50 Human Exomes Reveals Adaptation to High Altitude. *Science* **329**,
713 75–78 (2010).
- 714 46. Sabeti, P. C. *et al.* Genome-wide detection and characterization of positive selection in human
715 populations. *Nature* **449**, 913–918 (2007).
- 716 47. Szpiech, Z. A. & Hernandez, R. D. selscan: an efficient multithreaded program to perform EHH-
717 based scans for positive selection. *Mol Biol Evol* **31**, 2824–2827 (2014).
- 718 48. Lopez, M. *et al.* Genomic Evidence for Local Adaptation of Hunter-Gatherers to the African
719 Rainforest. *Current Biology* **29**, 2926-2935.e4 (2019).
- 720 49. Speidel, L., Forest, M., Shi, S. & Myers, S. R. A method for genome-wide genealogy estimation for
721 thousands of samples. *Nature Genetics* **51**, 1321–1329 (2019).
- 722 50. Stern, A. J., Wilton, P. R. & Nielsen, R. An approximate full-likelihood method for inferring
723 selection and allele frequency trajectories from DNA sequence data. *PLOS Genetics* **15**, e1008384
724 (2019).
- 725 51. Pan-UKB team. <https://pan.ukbb.broadinstitute.org> (2020).

- 726 52. Zhou, X. & Stephens, M. Genome-wide efficient mixed-model analysis for association studies.
727 *Nat Genet* **44**, 821–824 (2012).
- 728 53. Benjamini, Y. & Hochberg, Y. Controlling the False Discovery Rate: A Practical and Powerful
729 Approach to Multiple Testing. *Journal of the Royal Statistical Society. Series B (Methodological)*
730 **57**, 289–300 (1995).
- 731 54. Yekutieli, D. & Benjamini, Y. Resampling-based false discovery rate controlling multiple test
732 procedures for correlated test statistics. *Journal of Statistical Planning and Inference* **82**, 171–196
733 (1999).
- 734 55. Marnetto, D. & Huerta-Sánchez, E. Haplostrips: revealing population structure through haplotype
735 visualization. *Methods in Ecology and Evolution* **8**, 1389–1392 (2017).
- 736 56. Prüfer, K. *et al.* The complete genome sequence of a Neandertal from the Altai Mountains.
737 *Nature* **505**, 43–49 (2014).
- 738 57. Meyer, M. *et al.* A High-Coverage Genome Sequence from an Archaic Denisovan Individual.
739 *Science* **338**, 222–226 (2012).
- 740 58. Prüfer, K. *et al.* A high-coverage Neandertal genome from Vindija Cave in Croatia. *Science* **358**,
741 655–658 (2017).
- 742 59. Lonsdale, J. *et al.* The Genotype-Tissue Expression (GTEx) project. *Nat Genet* **45**, 580–585 (2013).
- 743 60. Kundaje, A. *et al.* Integrative analysis of 111 reference human epigenomes. *Nature* **518**, 317–30
744 (2015).
- 745 61. McLaren, W. *et al.* The Ensembl Variant Effect Predictor. *Genome Biology* **17**, 122 (2016).
- 746 62. Godyna, S., Diaz-Ricart, M. & Argraves, W. Fibulin-1 mediates platelet adhesion via a bridge of
747 fibrinogen. *Blood* **88**, 2569–2577 (1996).
- 748 63. Gudjonsson, A. *et al.* A genome-wide association study of serum proteins reveals shared loci with
749 common diseases. *Nat Commun* **13**, 480 (2022).
- 750 64. Rasmussen, A. H., Rasmussen, H. B. & Silaharoglu, A. The DLGAP family: neuronal expression,
751 function and role in brain disorders. *Molecular Brain* **10**, 43 (2017).

- 752 65. Trowsdale, J. & Knight, J. C. Major Histocompatibility Complex Genomics and Human Disease.
753 *Annual Review of Genomics and Human Genetics* **14**, 301–323 (2013).
- 754 66. Peng, C. *et al.* LRIG3 Suppresses Angiogenesis by Regulating the PI3K/AKT/VEGFA Signaling
755 Pathway in Glioma. *Frontiers in Oncology* **11**, (2021).
- 756 67. Zhou, H. *et al.* Member Domain 3 (LRIG3) Activates Hypoxia-Inducible Factor-1 α /Vascular
757 Endothelial Growth Factor (HIF-1 α /VEGF) Pathway to Inhibit the Growth of Bone Marrow
758 Mesenchymal Stem Cells in Glioma. *J biomater tissue eng* **11**, 1022–1027 (2021).
- 759 68. Bai, Z., Xu, L., Dai, Y., Yuan, Q. & Zhou, Z. ECM2 and GLT8D2 in human pulmonary artery
760 hypertension: fruits from weighted gene co-expression network analysis. *J Thorac Dis* **13**, 2242–
761 2254 (2021).
- 762 69. Takahashi, Y. *et al.* A genome-wide association study identifies a novel candidate locus at the
763 DLGAP1 gene with susceptibility to resistant hypertension in the Japanese population. *Sci Rep*
764 **11**, 19497 (2021).
- 765 70. Hansen, K. B. *et al.* PTPRG is an ischemia risk locus essential for HCO₃—dependent regulation of
766 endothelial function and tissue perfusion. *eLife* **9**, e57553.
- 767 71. Adeyemo, A. *et al.* A Genome-Wide Association Study of Hypertension and Blood Pressure in
768 African Americans. *PLOS Genetics* **5**, e1000564 (2009).
- 769 72. Slade, C. D., Reagin, K. L., Lakshmanan, H. G., Klonowski, K. D. & Watford, W. T. Placenta-specific
770 8 limits IFN γ production by CD4 T cells in vitro and promotes establishment of influenza-specific
771 CD8 T cells in vivo. *PLOS ONE* **15**, e0235706 (2020).
- 772 73. Long, L. *et al.* CRISPR screens unveil signal hubs for nutrient licensing of T cell immunity. *Nature*
773 **600**, 308–313 (2021).
- 774 74. Shinohara, T., Taniwaki, M., Ishida, Y., Kawaichi, M. & Honjo, T. Structure and Chromosomal
775 Localization of the Human PD-1 Gene (PDCD1). *Genomics* **23**, 704–706 (1994).
- 776 75. Liu, R., King, A., Tarlinton, D. & Heierhorst, J. The ASCIZ-DYNLL1 Axis Is Essential for TLR4-
777 Mediated Antibody Responses and NF- κ B Pathway Activation. *Mol Cell Biol* **41**, e0025121 (2021).

- 778 76. Tretina, K., Park, E.-S., Maminska, A. & MacMicking, J. D. Interferon-induced guanylate-binding
779 proteins: Guardians of host defense in health and disease. *J Exp Med* **216**, 482–500 (2019).
- 780 77. Mathieson, I. The omnigenic model and polygenic prediction of complex traits. *The American*
781 *Journal of Human Genetics* **108**, 1558–1563 (2021).
- 782 78. Mafessoni, F. *et al.* A high-coverage Neandertal genome from Chagyrskaya Cave. *Proceedings of*
783 *the National Academy of Sciences* **117**, 15132–15136 (2020).
- 784 79. Lee, J. H. *et al.* Further examination of the candidate genes in chromosome 12p13 locus for late-
785 onset Alzheimer disease. *Neurogenetics* **9**, 127–138 (2008).
- 786 80. Li, Y., Chu, L. W., Li, Z., Yik, P.-Y. & Song, Y.-Q. A Study on the Association of the Chromosome
787 12p13 Locus with Sporadic Late-Onset Alzheimer’s Disease in Chinese. *DEM* **27**, 508–512 (2009).
- 788 81. Sanders, S. J. *et al.* De novo mutations revealed by whole-exome sequencing are strongly
789 associated with autism. *Nature* **485**, 237–241 (2012).
- 790 82. Zhang, P. *et al.* Non-SMC condensin I complex, subunit D2 gene polymorphisms are associated
791 with Parkinson’s disease: a Han Chinese study. *Genome* **57**, 253–257 (2014).
- 792 83. Eichstaedt, C. A. *et al.* Genetic and phenotypic differentiation of an Andean intermediate altitude
793 population. *Physiol Rep* **3**, e12376 (2015).
- 794 84. Rimoldi, S. F. *et al.* Acute and Chronic Altitude-Induced Cognitive Dysfunction in Children
795 and Adolescents. *The Journal of Pediatrics* **169**, 238–243 (2016).
- 796 85. Yan, X., Zhang, J., Shi, J., Gong, Q. & Weng, X. Cerebral and functional adaptation with chronic
797 hypoxia exposure: A multi-modal MRI study. *Brain Research* **1348**, 21–29 (2010).
- 798 86. Chen, X. *et al.* Cognitive and neuroimaging changes in healthy immigrants upon relocation to a
799 high altitude: A panel study. *Human Brain Mapping* **38**, 3865–3877 (2017).
- 800 87. Turner, R. E. F., Gatterer, H., Falla, M. & Lawley, J. S. High-altitude cerebral edema: its own entity
801 or end-stage acute mountain sickness? *Journal of Applied Physiology* **131**, 313–325 (2021).

- 802 88. Inoue, T., Iseki, K., Iseki, C. & Kinjo, K. Elevated Resting Heart Rate Is Associated With White
803 Blood Cell Count in Middle-Aged and Elderly Individuals Without Apparent Cardiovascular
804 Disease. *Angiology* **63**, 541–546 (2012).
- 805 89. Apinjoh, T. O. *et al.* Association of candidate gene polymorphisms and TGF-beta/IL-10 levels with
806 malaria in three regions of Cameroon: a case–control study. *Malaria Journal* **13**, 236 (2014).
807